DOE/JPL/956615-84/3
(DE85001706)

LASER-ASSISTED SOLAR CELL METALLIZATION PROCESSING

Quarterly Report for the Period March 13—June 12, 1984

By
S. Dutta
P. G. McMullin

August 20, 1984

Work Performed Under Contract No. NAS-7-100-956615

Westinghouse R&D Center
Pittsburgh, Pennsylvania

Technical Information Center
Office of Scientific and Technical Information
United States Department of Energy

DISCLAIMER

DOE/JPL/956615-84/3
(DE85001706)
Distribution Category UC-63b

LASER-ASSISTED SOLAR CELL METALLIZATION PROCESSING

S. Dutta and P. G. McMullin

Quarterly Report for the period March 13
to June 12, 1984

Jet Propulsion Laboratory
Contract No. 956615

August 20, 1984

Westinghouse R&D Center
1310 Beulah Road
Pittsburgh, Pennsylvania 15235

CONTENTS

LIST OF FIGURES

ABSTRACT

Laser-assisted processing techniques, utilized to produce fine, metal grid patterns for high-efficiency solar cells, are being investigated, developed, and characterized. The work performed in the third quarter of this contract is detailed here. A preliminary economic evaluation has yielded the conclusion that laser-assisted pyrolysis of spun-on silver neodecanoate is the most promising of all the metallization techniques being investigated in this contract. Early adhesion problems have been solved by optimizing deposition parameters. Linewidth studies have been carried out as a function of laser power, scan speed, and film thickness. Preliminary solar cells have been fabricated and characterized using this metallization scheme. Silver neodecanoate films have also been decomposed using a pulsed UV laser and metal mask. A detailed study of the various models of localized surface temperature rise in silicon due to laser heating has been carried out. A review of this study and calculations of the silicon temperature rise resulting in decomposition of the spun-on silver neodecanoate are presented here.

1. SUMMARY

In this contract, laser-assisted processing techniques, utilized to produce fine, metal grid patterns for high-efficiency solar cells, are being investigated, developed, and characterized. The tasks comprising these investigations are outlined in the milestone chart shown in Figure 1.

During the first two quarters of this contract, preliminary investigations were carried out on several promising laser-assisted metallization schemes. A comprehensive literature search yielded information on state-of-the-art laser-assisted techniques for metal deposition such as laser chemical vapor deposition and laser photolysis of organometallics, as well as laser-enhanced electroplating. A compact system for the laser-assisted photolysis of gas-phase compounds was designed and constructed. Initial experiments on laser-enhanced electroplating yielded very promising results with linewidths as narrow as 25 μm and plating speeds as high as 12 μm/s being achieved. Metal deposition experiments were carried out utilizing laser-assisted pyrolysis of a variety of metal-bearing polymer films and metallo-organic inks spun onto silicon substrates. Argon-ion laser decomposition of spun-on silver neodecanoate ink, a generic metallo-organic ink synthesized by Professors G. M. and R. W. Vest of Purdue University, yielded fine, adherent silver lines. Solar cell comb metallization patterns were written using this technique, each pattern being written in a fraction of a second.

The work performed in the third quarter is detailed in this report. A preliminary economic evaluation has yielded the conclusion that laser-assisted pyrolysis of spun-on silver neodecanoate is the most promising of all the metallization techniques being investigated in this

Tasks/Milestones	1983 S O N D	1984 J F M A M J J A S
1. Conduct literature search on current state-of-the-art laser metallization schemes.	▬▬▲	
2. Assemble and test each of the following systems:		
2.1 Photolytic metal deposition using a focused CW UV laser.	▬▬▬▬▬▬▬▬▲	
2.2 Photolytic metal deposition using a mask and UV flood illumination.	▬▬▬▬▬▬▬▬▲	
2.3 Pyrolytic metal deposition using a focused CW laser.	▬▬▬▬▬▬▲	
3. Fabricate fifty solar cells.	▬▬▬▬▬▬▬▬▬▬▬▬▲	
4. Characterize the cells and determine the effects of transient heat on solar cell junctions and on bulk lifetime.	▬▬▬▬▬▬▬▬▬▬▬▬▲	
5. Compare economics of laser-assisted processing with competing technologies		
Preliminary Report	▲	
Final Report		Δ
6. Support Meetings	As Directed by JPL	
7. Provide Documentation	▬▬▬▬▬▬▬▬▬▬▬▬▬▬▬▬▬▬▬▬▬▬▬▬▬▬▬▬▬▬	

Figure 1. Milestone Chart

contract. Accordingly, maximum effort has been directed towards the development of this technique. Early adhesion problems have been solved by optimizing deposition conditions. Linewidth studies have been carried out as a function of laser power, scan speed, and film thickness. Preliminary solar cells have been fabricated and characterized using this metallization scheme. Silver neodecanoate films have also been decomposed using a pulsed UV laser and metal mask. A detailed study of the various models of localized surface temperature rise in silicon due to laser heating has been carried out. A review of this study and calculations of the silicon temperature rise resulting in decomposition of the spun-on silver neodecanoate are presented here.

2. RESULTS AND DISCUSSION

2.1 CW Argon-Ion Laser Pyrolysis of Silver Neodecanoate

A preliminary economic evaluation indicated that the metal deposition scheme involving the localized pyrolytic decomposition by a CW argon-ion laser of a silver neodecanoate film spun onto a silicon substrate, shown schematically in Figure 2, was the most promising of all the techniques under investigation. The low deposition rates obtained from laser decomposition of gas-phase compounds that are reported in the literature[1] would result in poor economic feasibility. This initial evaluation led to a decision to de-emphasize the experiments involving laser photolysis of gas-phase organometallics and place maximum emphasis on developing the laser pyrolysis of spun-on silver neodecanoate.

Significant progress has been achieved in the development of argon-ion laser decomposition of silver neodecanoate films spun onto silicon substrates. We had reported problems associated with adhesion of the deposited silver to silicon in the previous quarterly report. Heating the substrate to 100°C during laser decomposition provided better adhesion, but the deposited silver still failed the Scotch tape test. We wish to report that, using a combination of elevated substrate temperature and higher laser powers, we have deposited silver lines as fine as 10 μm with excellent adhesion to silicon.

The deposited lines easily withstand the Scotch tape test, as shown in Figure 3(a). This shows a 200X Nomarski photomicrograph of a silver line written at 4 W using a scan speed of 20 cm/sec and a substrate temperature of 75°C, before and after the Scotch tape test, tape having been applied to and pulled away from the right-hand side of the line. The Gaussian power distribution of the laser spot has resulted in a central deposit of silver, tapering off to carbon deposits

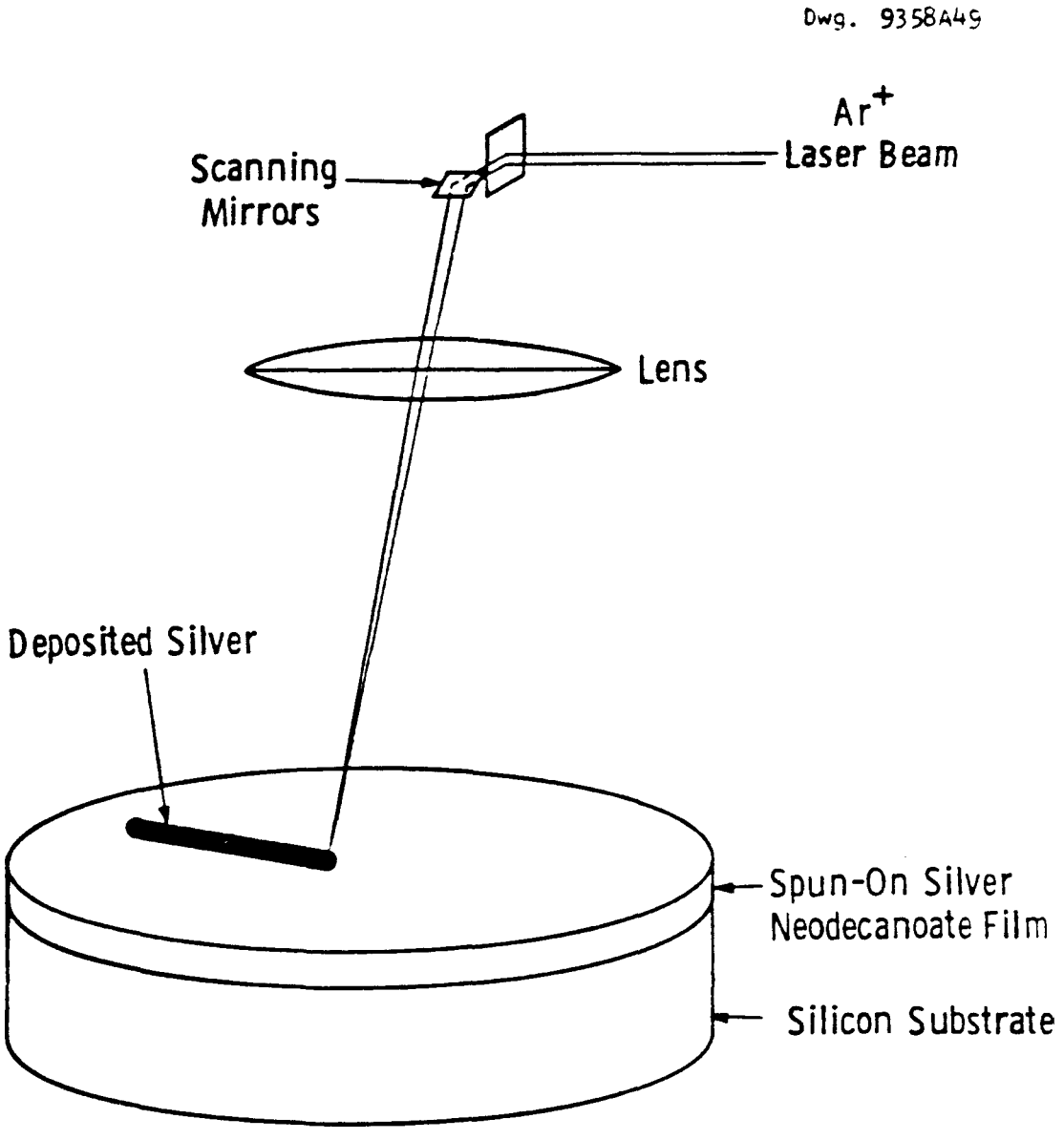

Figure 2. Schematic of experimental set-up for laser pyrolysis of spun-on metallo-organic films.

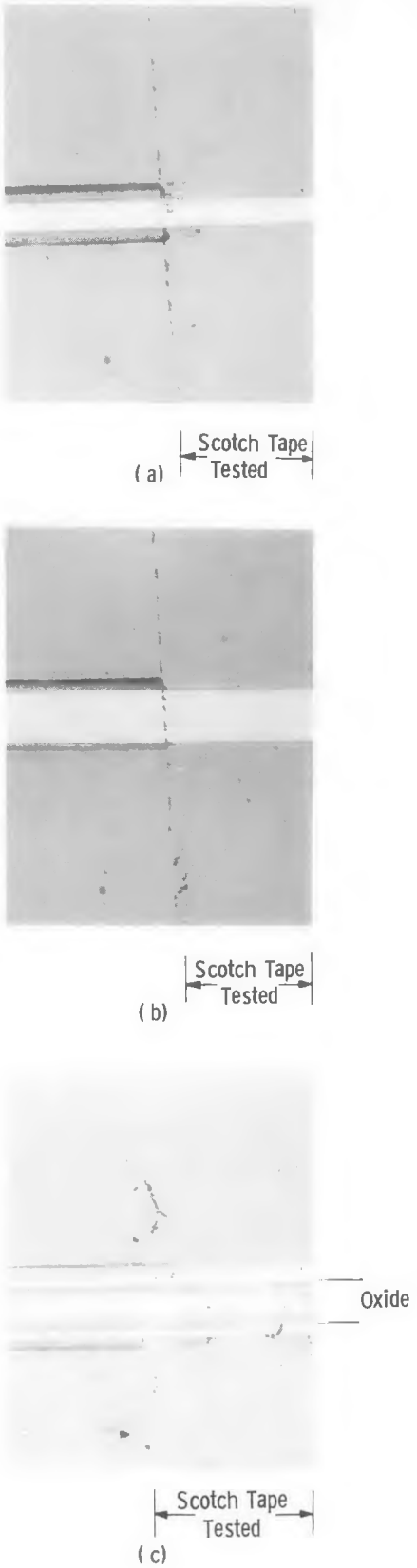

Figure 3. 200X Nomarski micrographs of silver lines decomposed at (a) 4W, (b) 8W, and (c) 14W, before and after the Scotch tape test.

at the edges of the line, where the laser power, and, hence, the decomposition temperature, was lower. The Scotch tape removes the carbon deposits, leaving the central, dense, silver line. At higher powers there is very little carbon deposition at the edges, as shown in Figure 3(b), which shows a line written at 8W. At still higher powers, 14W, the central, hottest region oxidizes, the fringes remaining metallic silver, as shown in Figure 3(c).

A study of the dependence of linewidth and adhesion on laser power and substrate temperature has been carried out. Lines were written at laser powers ranging from 6 W to 14 W at room temperature, 50°C, and 75°C, at a scan speed of 20 cm/s. The results are summarized in the graph shown in Figure 4. The linewidths shown are those obtained after a scrub to remove any carbon deposits around the edges. The open symbols denote lack of adhesion. It may be seen that linewidth increases almost linearly with laser power and is not dependent upon substrate temperature. Adhesion improves at higher laser powers as well as at elevated substrate temperatures.

The effect of scan speed on deposited linewidth has also been studied for a wide range of laser powers. Lines were written at scan speeds of 0.2 cm/s, 2 cm/s, and 20 cm/s at laser powers ranging from 2 to 16 W. The substrate temperature was held fixed at 75°C. The results of this study are plotted in the graph shown in Figure 5. The open symbols at higher powers indicate oxidation of the metal, and the dotted symbols at the lowest scan speed and highest powers denote alloying of the silver with silicon. The increased dwell time during slow scans results in wider lines, as expected. Linewidths as fine as 10 μm may be obtained by using rapid scans and low laser powers. The silver deposits at such low powers look grainy, however, and are not as adherent.

2.2 Laser-Metallized Solar Cells

Twelve 1 x 1 cm^2 solar cell comb metallization patterns were directly written on a diffused silicon wafer by argon-ion laser

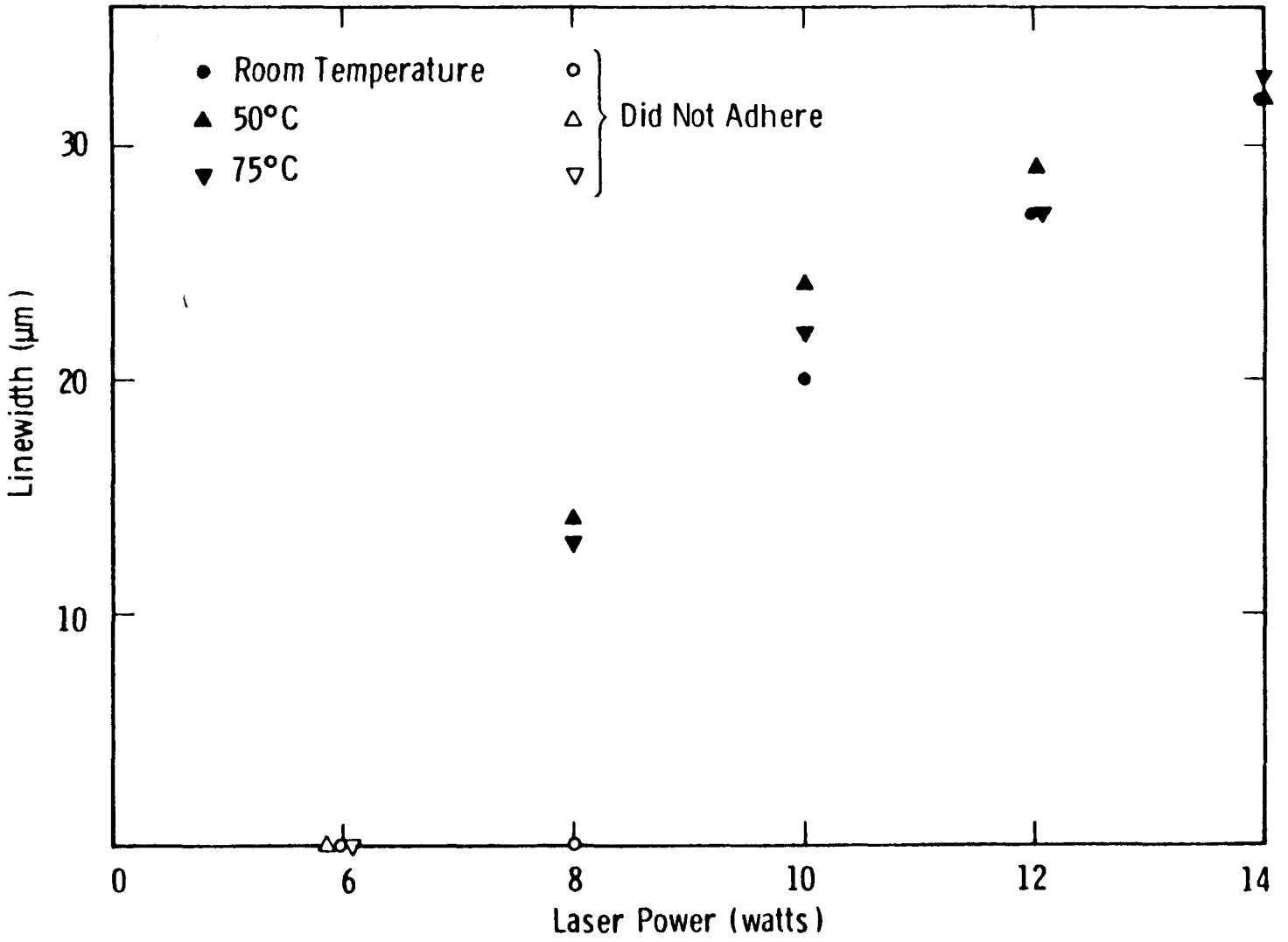

Figure 4. Laser-written linewidths plotted as a function of laser power and substrate temperature.

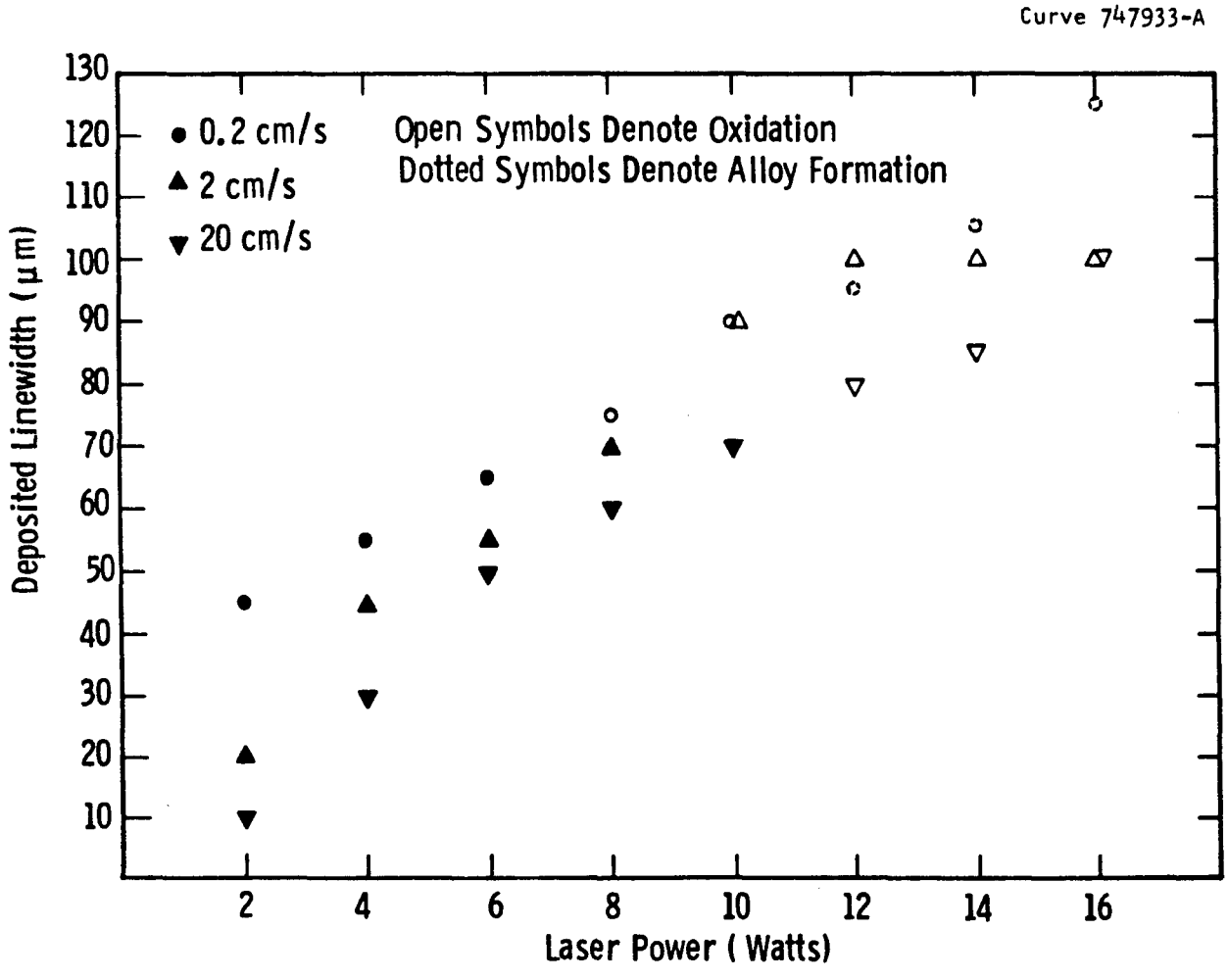

Figure 5. Deposited linewidths as a function of scan speed and laser power.

decomposition of spun-on silver neodecanoate. Figure 6 shows an example of laser-written comb patterns on a previous wafer.

Silver neodecanoate powder obtained from Purdue University was dissolved in xylene and spun at 1000 rpm onto the front surface of a two-inch diffused silicon wafer. The optimized experimental conditions for depositing adherent, fine silver lines, as determined from the experiments detailed in the previous section, were used. The 9 mm long teeth and connecting line of the comb were written with single laser scans at a laser power of 12 W and a scan velocity of 20 cm/s, using a substrate temperature of 75°C. The 2 mm x 1 mm contact pads were written using a laser power of 3 W and a scan overlap of 60%. The laser power was cut down to 3 W for the contact pads because the previous experiments indicated a "blooming" of the film around contact pads written at higher laser powers, as can be seen in Figure 6.

After the patterns were written, the unexposed parts of the film were rinsed away in acetone. To obtain a back contact, silver neodecanoate was spun onto the back of the wafer and decomposed into silver by placing the wafer on a hot plate. The metal thickness on both front and back was then built up to 5 μm, the required current-carrying thickness, by electroplating. It was seen that the contact pads adhered poorly. Adhesion of the pads was not improved by sintering at 450°C in H_2 for 30 minutes.

The solar cells were laser scribed and tested. The lighted current-voltage characteristics of one of the cells is shown in Figure 7. The open-circuit voltage is 0.564 V, the short-circuit current is 25.47 mA, the resistance of a unit area cell is 0.51 ohm-cm^2, and the fill factor is 0.527, yielding a non-AR-coated cell efficiency of 7.6%. The normalized series resistance obtained from the dark I-V characteristics was found to be a factor of ten higher than normal. This high series resistance, indicative of high contact resistance, is primarily responsible for the low fill factor, leading to the relatively low cell efficiency obtained. This high contact resistance is due to

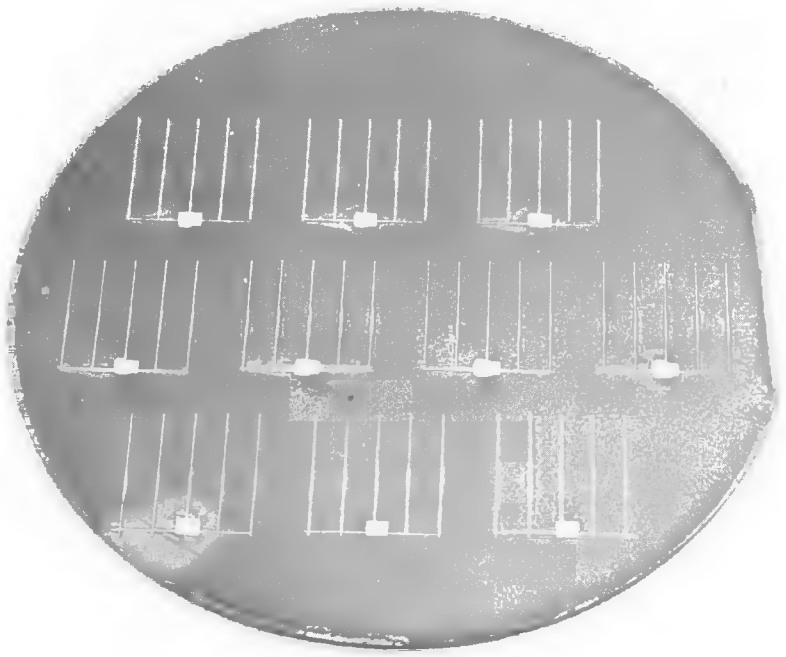

Figure 6. Laser-written solar cell metallization patterns using spin-on silver neodecanoate.

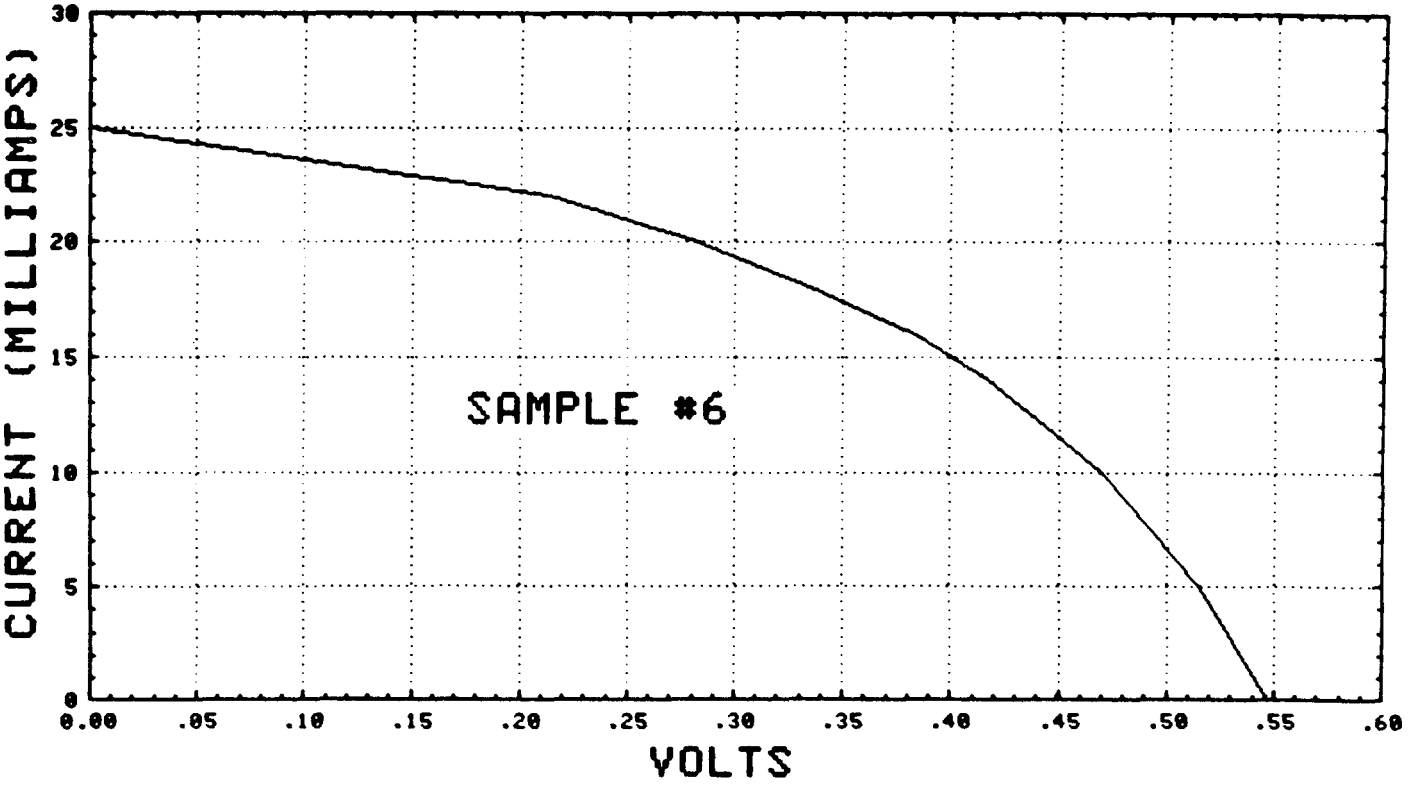

Laser Metallization Conditions

Lines: Laser Power = 12W
Single Scan
Contact Pads: Laser Power = 3W
Scan Overlap = 60%
Substrate Temperature = 50°C

Non - Ar - Coated
Cell Efficiency = 7.6%

Figure 7. Current-voltage characteristics of laser-metallized solar cell.

poor adhesion of the contact pads, which were written at a low laser power of 3 W. Experiments utilizing conditions leading to improved contact resistance have resulted in high-quality cells. Details of these new experiments will be reported on in the next quarterly report.

2.3 Pulsed UV Laser Pyrolysis of Silver Neodecanoate

Silver neodecanoate films spun onto silicon substrates were decomposed using a pulsed UV laser. A tripled Nd:YAG laser operating at 335 nm with a maximum energy of 100 mJ, pulse width of 6 ns, and pulse repetition rate of 10 Hz was used. The doughnut-shaped beam size was 6 mm. In our preliminary experiments a metal mask with an array of dot apertures was placed in front of the wafer. No substrate heating was used. The wafer was exposed to the laser at maximum energy, 100 mJ, for a total of 15 seconds, corresponding to 150 pulses. The silver dots deposited through the mask had excellent definition. After the unexposed parts of the film were rinsed away in acetone, it was observed that the deposited silver had adhered only in the regions of highest laser intensity. Underneath the silver dots that had been rinsed away, darkened dots of silicon were observed, indicating that some laser damage had occurred. Further experiments with the UV laser are planned, using beam aperturing.

2.4 Review of Temperature Rise Models

A calculation of the surface temperature rise produced by a scanning laser beam must take into account the Gaussian intensity profile of the laser beam, the temperature-dependent thermal conductivity of the silicon substrates, the substrate temperature, the absorption length of the laser light in the silicon, and the effect of scanning velocity. In the following sections, each of these factors will be analyzed in turn.

The response of a semi-infinite solid to heating by a stationary Gaussian beam has been examined by Lax[2] and Bass.[3] Nissim et al.[4]

have extended the analysis to Gaussian beams with elliptical intensity contours. Each of these authors presents an expression for the maximum temperature reached at the surface of the silicon at the center of the laser beam. The maximum temperature is a quantity of interest in itself and is also used to normalize the general solutions for easier study of the spatial dependences. Their expressions are compared below:

(1)	Lax[2]	$T_{max} = P/[2\sqrt{\pi}\,Kw]$	(equations 1.3, 1.4, 3.8)
(2)	Bass[3]	$T_{max} = \alpha P_o/[2\,K\sqrt{\pi}\,w]$	(p. 95)
(3)	Nissim[4]	$\Theta = p/[C_p\,D\,2\sqrt{2\pi}]$	(equation 15)

The apparent discrepancies are resolved as follows. Bass defines α as the fraction of incident power which enters the sample,[5] while P_o is the incident power in the laser beam, giving the identity $P = \alpha P_o$ since Lax has defined P directly as the power entering the sample. Nissim has used a parameter p given by

$$p = P\,(1-R)/r_x$$

where P is the incident power, R is the reflectivity, and r_x is the Gaussian beam radius. Thus, P(1-R) is the power entering the sample in agreement with Lax and Bass. The Gaussian radius r_x defined by Nissim differs from the radius w chosen by Lax and Bass in the following way.

Nissim	$I = I_o \exp\,[-r^2/2\,r_x^2]$
Lax, Bass	$I = I_o \exp\,[-r^2/w^2]$

According to Nissim, at the beam radius r_x, the intensity of the beam is decreased by exp[-1/2] compared to the beam center, while according to the others, at the beam radius w the intensity is down by exp[-1] compared to the center. This accounts for a factor of $\sqrt{2}$ in the denominator of Nissim's expression. Finally, we have

$$K = C_p D$$

where K is the thermal conductivity, C_p is the volume specific heat, and D is the thermal diffusivity. The three authors are thus in complete agreement for this case.

The equivalent expressions listed above give the temperature in the center of a Gaussian spot at the surface of a semi-infinite solid for which the thermal conductivity is constant. This is a good approximation for the metals and other materials considered by Bass but is not accurate for silicon. The thermal conductivity of silicon, and of semiconductors generally, is a strong function of temperature. A mathematical method to deal with a varying thermal conductivity is shown in a second paper by Lax.[6] A "linear" temperature Θ is defined, which is related to the true temperature T by a Kirchhoff integral transform:

$$\Theta(T) = \int_{T_o}^{T} K(T)/K(T_o)\, dT \tag{4}$$

where K(T) is the thermal conductivity as a function of temperature and T_o is the substrate ambient temperature. The linear temperature Θ obeys the heat equation with constant $K = K(T_o)$. Thus, the maximum <u>linear</u> temperature is given by expressions (1)-(3) and the true maximum temperature is found by inverting the transformation in expression (4). Nissim et al.[4] describe the thermal conductivity of silicon by the expression

$$K(T) = A/(T-B) \tag{5}$$

where $A = 299^{o}K$, $B = 99^{o}K$, and T is the true local temperature in Kelvins. With this particular form, the integral in (4) may be evaluated analytically, and the relation may be solved for T to give

$$(T-T_o) = (T_o-B)\,(\exp\,[\Theta/(T_o-B)] - 1) \tag{6}$$

Because of the exponential form, the true temperature rise will always exceed the linear temperature rise. In physical terms, the thermal conductivity of silicon is a decreasing function of temperature, so the application of a heat input causes a decrease in the conductivity, thereby accelerating the temperature rise.

To illustrate the difference between the linear and true temperature rises, Table 1 shows the predicted maximum temperature rises for a range of heat inputs. The input power is expressed as the total power entering the substrate divided by the Gaussian beam radius. (The beam radius definition r_x of Nissim is used: to convert to the definition w of Lax and Bass, divide all input powers by the square root of two.) The linear temperature rise is computed from expressions (1)-(3) using the thermal conductivity at the substrate temperature ($25^{\circ}C$) as given by expression (5). The true temperature rise is computed from expression (6). It can be seen that for input powers exceeding 2 kW/cm, the true temperature rise is greater than twice the linear temperature rise. The effect of the temperature dependence of the thermal conductivity is a major factor in computing the temperature rise and should be included even for low and moderate power inputs.

The maximum linear temperature rise in expressions (1)-(3) was derived assuming the input power is dissipated at the surface. For optical heating, the power is actually spread over an absorption length $1/\alpha$, where α is the wavelength-dependent absorption length of the substrate. The effect of a finite absorption length has been shown by Lax,[2] where complete mathematical forms and asymptotic expressions are given. However, the exact expressions are unwieldy and difficult to use. An approximation may be derived based on Lax's Figure 1. The absorption length in silicon at the principal wavelength of the argon-ion laser (488 and 504 nm) is about 600 nm, based on the recent data of Aspnes and Studna.[7] Assuming a Gaussian spot diameter of 15 μm or greater, this gives a normalized parameter $W = \alpha w$ of 25 or more. From Figure 1, this corresponds to a decrease of about five percent or less of the maximum linear temperature.

Table 1. Temperature Rise of a Silicon Wafer by a Gaussian Laser Spot, According to the Model of Nissim et al., with a Substrate Temperature of 25°C

INPUT POWER WATTS/CM	TRUE TEMPERATURE RISE	LINEAR TEMPERATURE RISE
100	13.7	13.3
200	28.4	26.6
300	44.1	39.8
400	60.9	53.1
500	78.8	66.4
600	98.0	79.7
700	118.4	92.9
800	140.3	106.2
900	163.8	119.5
1000	188.8	132.8
1100	215.5	146.0
1200	244.1	159.3
1300	274.7	172.6
1400	307.4	185.9
1500	342.3	199.1
1600	379.7	212.4
1700	419.6	225.7
1800	462.3	239.0
1900	507.9	252.2
2000	556.6	265.5
2100	608.8	278.8
2200	664.5	292.1
2300	724.1	305.3
2400	787.7	318.6
2500	855.8	331.9
2600	928.6	345.2
2700	1006.4	358.4
2800	1089.5	371.7
2900	1178.4	385.0
3000	1273.5	398.3
3100	1375.0	411.6
3200	1483.6	424.8
3300	1599.7	438.1
3400	1723.8	451.4
3500	1856.5	464.7

The effect of scanning velocity on the temperature rise was considered by Nissim et al.[4] The expressions they derived are based on a Green's function solution which includes the thermal diffusivity D as a parameter. The diffusivity is proportional to the thermal conductivity, which is a strong function of temperature. Nissim makes no attempt to account for this temperature dependency, and indeed it may not be possible to give an analytical solution in closed form with such a non-linear temperature-dependent parameter. However, the results of Nissim can serve as a guide to the effect of scanning velocity and should be reasonably accurate for moderate temperature rises.

Nissim's results are given in terms of Θ normalized velocity V given by

$$V = v\, r_x/2D$$

where v is the scanning velocity in cm/s, r_x is the Gaussian beam radius in the definition of Nissim, and D is the thermal diffusivity. Using $K = DC_p$, with the volume specific heat C_p = 1.63 J/K cm^3, and thermal conductivity K = 1.5 W/cmK as computed from Nissim's expression (5), the thermal diffusivity at room temperature is D = .92 cm/s. In our experiments, v and r_x have the maximum values of 50 cm/s and 25 μm, respectively. Thus, V is typically 0.07 or less in our experiments. From Nissim's Figure 11, this corresponds to a five percent decrease in the maximum temperature, and from Figure 7 to a very slight distortion of the temperature distribution along the scanning direction. The conditions at the laser spot are therefore only slightly different from a stationary spot of a few percent less input power, in terms of the linear temperature. The corrections for optical absorption length and scanning velocity should be applied to the calculated linear temperature before taking the transformation (6) to find the true temperature.

The effects considered above can be accounted for by the parameters of the model. Additional effects must be considered before an accurate calculation can be made. The most important is the proper

calculation of the power entering the sample. This depends on the condition of the surface and on the nature of any surface coatings that might exist. The reflectivity of a damage-free silicon surface ranges from about 33 to 40 percent as a function of wavelength in the visible band. However, coatings on the surface can act as antireflection layers, substantially decreasing the reflectivity. The amount of reflectivity decrease depends on the index of refraction and the thickness of the coating. Also, the reflectivity depends on the temperature of the silicon. In particular, if localized melting occurs, there is a marked increase in reflectivity corresponding to the phase change. These effects must be evaluated according to the particular case under study.

2.5 Estimation of Temperature Rise in Solar Cell Writing Experiments

An argon-ion laser was used to decompose a silver neodecanoate film on the surface of a silicon wafer. The laser spot was scanned at 20 cm/s by means of mirrors mounted on galvanometers. The Gaussian beam spot size is estimated as 30 microns in diameter from the width of silicon melt lines in a separate experiment. The beam radius is taken as .0015 cm according to the definition of Nissim et al.[4] The output power of the laser was measured by directing a fraction of the beam from a calibrated beam splitter into a calorimetric detector. The laser output power ranged from 3 to 12 W. Between the laser output port and the solar cell sample, there are five dielectric mirrors with about .5 percent loss each, for a 2.5 percent total loss from reflection. The focussing lens is not antireflection coated and causes eight percent loss from surface reflections. Thus, the power reaching the sample is about ten percent less than the laser power.

The reflectivity of a bore, damage-free crystalline silicon surface at the argon-ion laser wavelengths (488 and 514 nm) is about 38 percent. The antireflection effect of the coating film is noticeable to the eye but has not been measured. The film can only cause a decrease in the reflectivity, since the index of the film is intermediate between that of air and silicon. We estimate the reflection loss at the surface

as 30 percent. The power entering the silicon substrate is thus about 60 percent of the total laser beam power, or 1.8 to 7.2 W in our experiments. Dividing by the Gaussian beam radius gives an input power parameter of 1200 to 4800 W/cm. The predicted linear temperature rise at 1200 W/cm input is 159°C for a substrate temperature of 25°C. The true temperature rise, taking account of the temperature dependence of the thermal conductivity, is 244°C, for a maximum temperature at the center of the laser spot of 269°C. This calculated temperature is consistent with our observation that power levels below 3 W do not cause decomposition of the film, which occurs at 250°C. The calculated linear and true temperature rises for 4800 W/cm power input parameters are 637 and 4694°C, respectively. This estimate is obviously too high, since 4694°C is well above the vaporization point of silicon, but no damage to the surface is observed. We believe that the deposition of a metallic silver layer at the leading edge of the laser spot increases the surface reflectivity so that relatively little power is absorbed from the center of the laser spot. In this sense, the silver deposition is a self-protecting process, since formation of the shiny metallic deposit prevents damage from laser overexposure.

3. CONCLUSIONS AND RECOMMENDATIONS

Direct writing of solar cell metallization patterns using CW argon-ion laser decomposition of spun-on silver neodecanoate films is proving to be a very promising metallization scheme. Early adhesion problems have been solved by using a combination of elevated substrate temperature and higher laser powers. This enabled us to write several solar cell comb patterns on a diffused silicon wafer and build up the metal thickness by subsequent electroplating. The contact pads, however, did not adhere very well, as they were written at lower laser powers to avoid "blooming" of the surrounding film. This led to a high contact resistance and low fill factor, yielding a relatively low non-AR-coated cell efficiency of 7.6%. We are currently exploring methods of improving the contact resistance and have obtained high-quality cells using these improved techniques. These experiments will be elaborated upon in the next report.

Deposition of silver using a pulsed UV laser and a mask was accomplished. Since there was no facility for heating the substrate, adhesion was poor except at the highest powers. Nonuniformity of the beam caused problems, so beam aperturing will be incorporated into the next series of experiments.

A calculation of the surface temperature rise produced by a scanning laser beam agreed fairly well with the experimental results at low laser powers. At higher powers, the high reflectivity of the deposited metal sharply reduces the power absorbed and, consequently, the surface temperature rise, so that there is a much greater discrepancy between calculated and experimental results. The oxidation of the metal observed at very high laser powers can probably be prevented by directing a jet of nitrogen over the wafer surface.

4. PROJECTION OF ACTIVITIES FOR FOURTH QUARTER

Laser-metallized solar cells with improved efficiencies will be fabricated and characterized. The resistivity and contact resistance of the deposited silver will be carefully measured. Techniques to reduce the contact resistance without degrading cell performance will be explored. Further experiments involving UV laser decomposition of silver neodecanoate through a mask will be conducted. Laser-enhanced electroplating will also be investigated in greater depth.

5. ACKNOWLEDGEMENTS

The authors with to thank D. W. Feldman for allowing them the use of his UV laser set-up and for his advice and assistance on the experiments performed there. The authors are indebted to W. E. Dooley for his assistance with the UV laser experiments, P. Palaschak and D. N. Schmidt for assistance with the adhesion and linewidth studies, J. B. McNally and P. Palaschak for solar cell fabrication and laser writing of the comb patterns, F. S. Youngk for electroplating of the cells, S. Karako for solar cell testing, G. S. Law for reading and preparing the manuscript, and M. G. Markle for typing the report.

6. REFERENCES

1. D. J. Ehrlich, R. M. Osgood, Jr., and T. F. Deutsch, "Photodeposition of Metal Films with Ultraviolet Laser Light," J. Vac. Sci. Technol., Vol. 21, pp. 23-32 (1982).

2. M. Lax, "Temperature Rise Induced by a Laser Beam," J. Appl. Phys., Vol. 48, pp. 3919-3924 (1977).

3. Michael Bass, "Laser Heating of Solids," in Physical Process in Laser-Materials Interactions, M. Bertolotti (ed.), Plenum 1980, pp. 77-115.

4. Y. I. Nissim, A. Lietoila, R. B. Gold, and J. F. Gibbons, "Temperature Distributions Produced in Semiconductors by a Scanning Elliptical or Circular CW Beam," J. Appl. Phys. Vol. 51, pp. 274-279 (1980).

5. See Ref. 2, pp. 81 and 99; α is dimensionless, contrary to listing on p. 114 as cm^{-1}.

6. M. Lax, "Temperature Rise Induced by a Laser Beam II: The Nonlinear Case," Appl. Phys. Lett., Vol. 33, pp. 786-788 (1978).

7. D. E. Aspnes and A. A. Studna, "Dielectric Functions and Optical Parameters of Si, G, GaP, GaAs, GaSb, InP, InAs, and InSb from 1.5 to 6.0 eV," Phys. Rev. B, Vol. 27, pp. 985-1009 (1983).

•U. S. GOVERNMENT PRINTING OFFICE: 1984-544-063/10396